

Supporting Information

Rhodium Metal-Rhodium oxide (Rh-Rh₂O₃) Nanostructures with Pt-like or Better Activity towards Hydrogen Evolution and Oxidation Reactions (HER, HOR) in Acid and Base: Correlating Its HOR/HER Activity with Hydrogen Binding Energy and Oxophilicity of the Catalyst

Manas Kumar Kundu[†], Ranjit Mishra[†], Tanmay Bhowmik and Sudip Barman*

School of Chemical Sciences, National Institute of Science Education and Research (NISER),
Bhubaneswar, Orissa - 751 005, India. E-mail: sbarman@niser.ac.in. Tel: +91(674)2494183

[†] Authors with equal contributions.

Materials:

Formamide (HCONH_2), 40% Platinum on carbon (comm. Pt/C) was purchased from Sigma-Aldrich. Rhodium (II) acetate ($\text{Rh}_2(\text{AcO})_4$, 98+% assay), Rhodium carbon (comm. Rh/C, 5%), sodium borohydride (NaBH_4) was purchased from Spectrochem (India). Sulfuric acid (H_2SO_4 , 98%) and potassium hydroxide (KOH), was bought from Merck (Germany). These all chemicals were used as they received without further purification. N_2 , H_2 and CO gases (99.99 % purity) were purchased from Sigma Aldrich. Mili-Q water was obtained from ultrafiltration system (Mili-Q, Millipore) with the measured conductivity 35 mho cm^{-1} at 25°C .

Experimental Section:

Synthesis of nitrogen-doped carbon:

Nitrogen doped carbon (CN_x) was synthesized by microwave heating of Formamide (HCONH_2), reported recently by our group¹. Briefly, a 30 ml volume of HCONH_2 was subjected to a microwave irradiation for 2h at 180°C & brown coloured solution was obtained. Then, the resulting solution was vacuum evaporated in a rotary evaporator at 180°C to produce nitrogen-doped carbon. Finally product was collected by filtration, then washed thoroughly with distilled water and dried under vacuum to get dry, solid nitrogen-doped carbon.

Preparation of the RhNPs/C composite:

RhNPs/C composite was synthesized via reduction of rhodium (II) acetate by NaBH_4 followed by ultrasonic treatment. Briefly, 55 mg of Rhodium (II) acetate was taken in 5 ml water & sonicated for 30 minutes to disperse it well. Then 46 mg of NaBH_4 was directly added into the solution and again sonicated properly. In another vial, 5 mg of as prepared of CN_x was dispersed in 2 ml water by sonication for few minutes. Then two solutions are

mixed together by using a bath-sonicator for 10 minutes. Finally resultant solution was sonicated by ultrasound operating at 28 kHz frequency (power 700 watt) for 180 minutes. The black coloured mass was recovered by centrifugation at 16,000 rpm for 20 minutes and washed repeatedly with deionized water & ethanol. Finally, the product was kept in vacuum for drying.

Synthesis of the Rh-Rh₂O₃-NPs/C nanostructures:

Rh-Rh₂O₃-NPs/C was synthesized by thermal heating of RhNPs/C. As prepared RhNPs/C composite was taken in an alumina crucible and calcinated at 450°C in a tube furnace with a temperature accuracy ± 2 °C for 4 h. After that, it was cooled down to room temperature normally & collected carefully black solid product.

For comparison purpose we have synthesized only Rh sample without using any carbon support, following the same synthesis procedure. This composite is termed as Rh-Rh₂O₃.

Characterizations:

For synthesis of nitrogen doped carbon, MAS-II microwave synthesizer was used and bought from SINEO Microwave Technology Company (Shanghai, China). Ultrasound treatment was carried out by SINEO UWave-1000 (Shanghai, China) with 28 kHz frequency. The powder x-ray diffraction pattern (p-XRD) of samples was performed by Bruker DAVINCI D8 ADVANCE diffractometer equipped with Cu K α radiation ($\lambda = 0.15406$ nm). Field-emission scanning electron microscope (FESEM) system (Carl Zeiss, Germany make, Model: Sigma) was used for taking FESEM images and FESEM samples were prepared by casting a drop on a Si-wafer and dried at air around 45°C. The surface morphology was investigated by Transmission Electron Microscopy (TEM, JEOL 2100F) operated at 200 kV. High-Resolution TEM (HRTEM) was also taken using same instrument. TEM samples were prepared by taking 10 μ l solutions from a stock 4×10^{-5} mg/l and dried at air around 45°C.

CHNS was analyzed by Euro Vector (Euro EA analyzer 3000). XPS measurements were done using VG Microtech where monochromatic Mg K_{α} X-ray was the source. XPS was taken from the sample deposited on Si wafer. Electrochemical measurements were performed with an Electrochemical Workstation (Autolab, Metrohm, PGSTAT 320N), equipped with rotating disk electrode (RDE). A conventional three-electrode system, glassy carbon as a working electrode, platinum wire as a counter electrode and Ag/AgCl as a reference electrode were used. In order to reduce noise in chronoamperometric measurements due to bubble accumulation, smoothing was applied in chronoamperometric responses where needed. pH of the working solution was measured before experiment by Hanna (HI 2209) pH meter.

Electrochemical measurements:

All the electrochemical measurements were done in a conventional three-electrode system at an Autolab 302 N electrochemical station using Ag/AgCl (3 M KCl) as reference electrode, Pt wire as counter electrode and glassy carbon (GC) as a working electrode. GC electrode was polished with 1.0, 0.1 and 0.05 mm alumina slurry on Buehler micro cloth polishing cloth. After rinsing with copious water, the electrode was sonicated in distilled water about 10 min. 1 mg of synthesized composite was dissolved in 1 ml water to make a stock solution. 2.5 μ l of aqueous stock solution was evaporated on cleaned glassy carbon electrode to prepare Rh-Rh₂O₃-NPs/C electrode. Thus amount of Rh on the GC electrode was calculated 2 μ g. For stability measurement 10 μ l 5 wt% nafion solution was used to make the stock solution and only in KOH medium 5 μ l of aqueous stock solution (i.e 4 μ g of Rh) was drop-casted on GC. The amount of comm. Pt/C and comm. Rh/C was also kept same for comparison for all the experiment. 10 μ l 5% nafion and 10 μ l ethanol was used to make the stock solution of comm. Pt/C and comm. Rh/C. Potential obtained from Ag/AgCl reference electrode was converted to RHE by using the general formula $E_{RHE} = E_{Ag/AgCl} + E^0_{Ag/AgCl} + (0.059 \times \text{pH})$, where $E_{Ag/AgCl}$ is the working potential, $E^0_{Ag/AgCl} = 0.1976$ at 25^oC (3 M KCl).

pH was also measured for all electrolyte before experiment. Thus the HER measurements were carried out in both acidic and basic medium degassed with nitrogen using LSV at a scan rate 10 mV/sec. HOR was done in different pH solutions with the help of linear sweep voltammetry (LSV) by using hydrogen 10 mV sec⁻¹ scan rate in a H₂ saturated environment. CV was done in different pH with 30 mv/sec scan rate with N₂ saturated medium. CO stripping measurement was performed by first holding the electrode potential at 0.1 V (RHE) for full monolayer adsorption of CO on metal surface. Then N₂ was flowed to remove the dissolved CO from the solution. Then CV scan was performed at 30 mV/sec where the forward scan represents the CO stripping. The stability of the electrode was measured by chronopotentiometric where a constant current was applied for certain time. AC impedance measurements were performed in the identical system in the frequency range 10⁵ Hz to 10⁻¹ Hz with a constant AC voltage. All HOR polarization curves in different pH were iR corrected. In impedance spectra linearly extrapolated intercept with real axis was taken as resistance of cell (solution) and this value was used for iR correction.

Structural characterization by Scherrer Equation:

The size of Rh-Rh₂O₃-NPs/C was determined from the following Debye–Scherrer Equation² described bellow

$$B(2\theta) = \frac{K\lambda}{L \cos \theta}$$

Where L is the mean size of the ordered (crystalline) domains, K is a dimensionless shape factor, with a value close to unity. The shape factor has a typical value of about 0.9, but varies with the actual shape of the crystallite, λ is the X-ray wavelength (0.154 nm), B is the line broadening at half the maximum intensity (FWHM) in radians. The most intense peak

positioned (2θ) at 40.91° was used to calculate the size of Rh-Rh₂O₃-NPs/C in the composite using above equation and obtained as 10 nm.

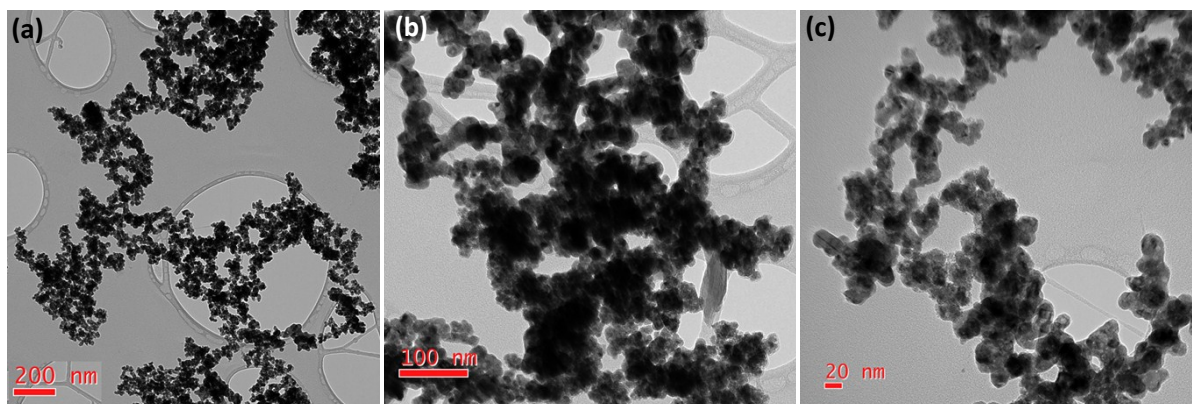


Figure S1. (a-c) TEM images of Rh-Rh₂O₃-NPs/C.

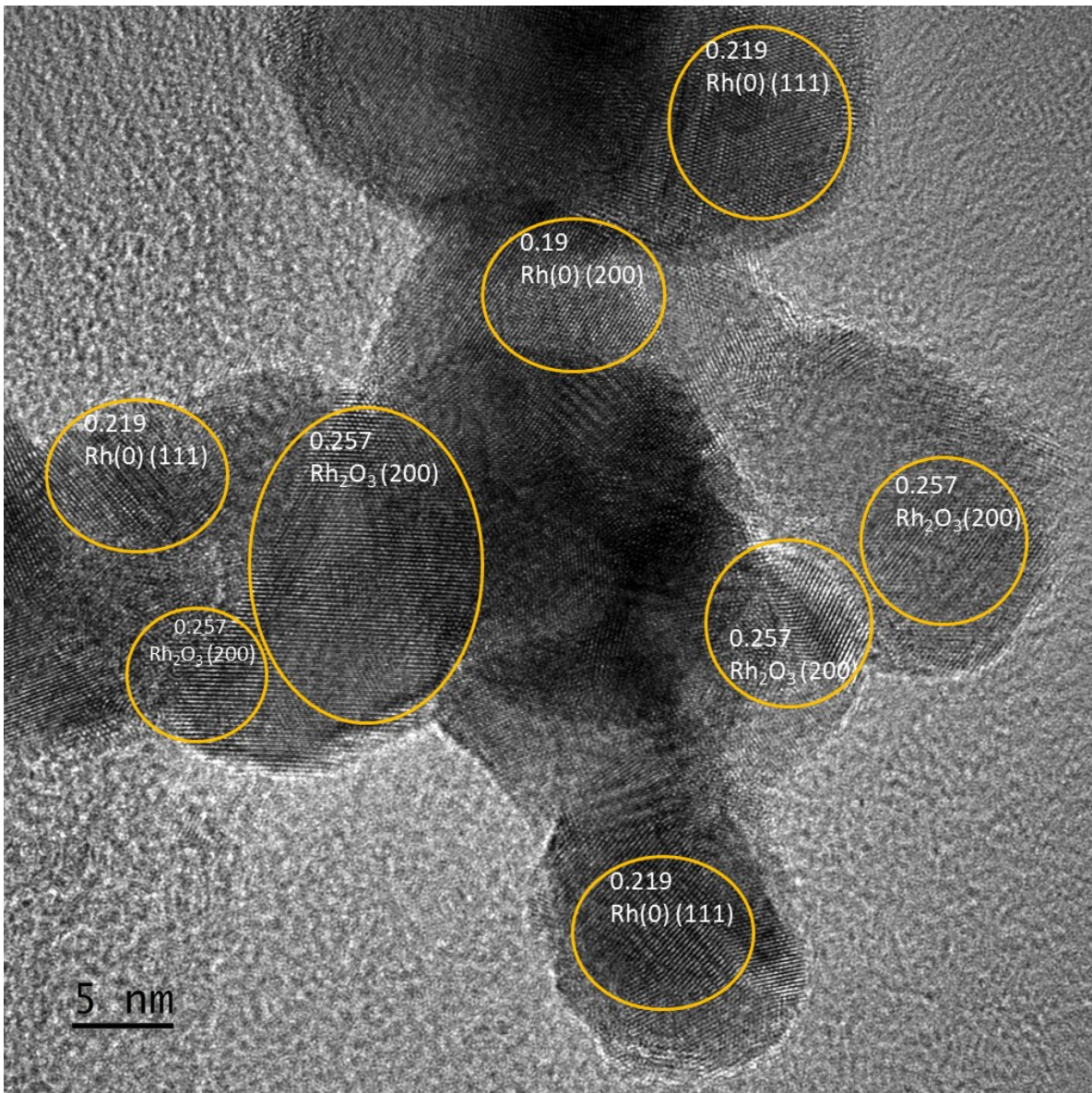


Figure S2. (a, b) HRTEM image of Rh-Rh₂O₃-NPs/C showing the presence of Rh (metal) and Rh₂O₃.

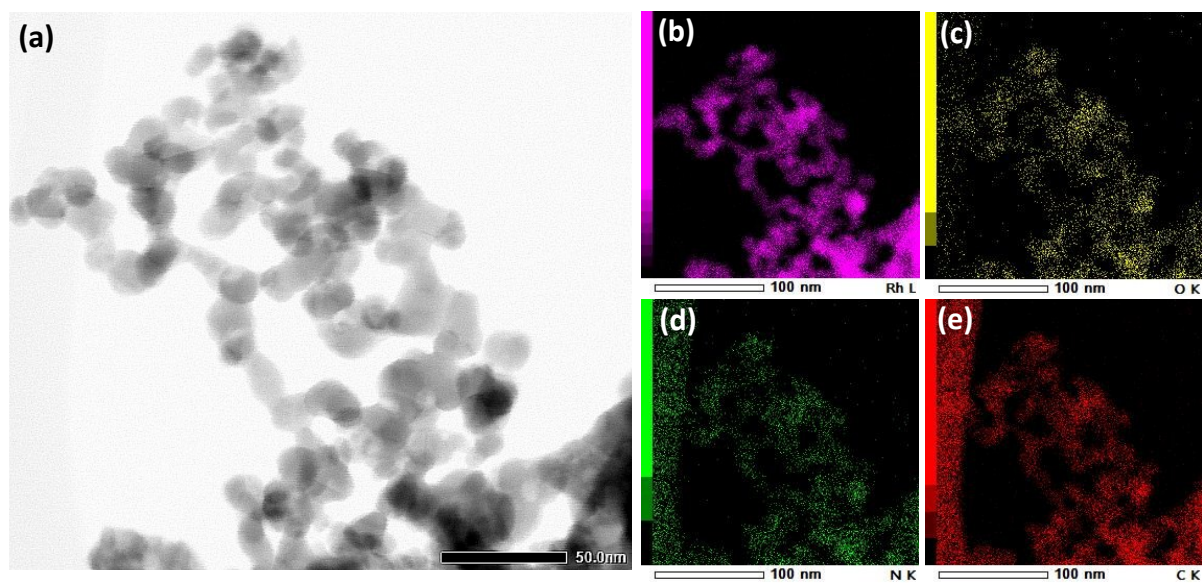


Figure S3. (a) STEM bright field image of Rh-Rh₂O₃-NPs/C composite. (b- e) Corresponding EDS elemental mapping of Rh, O, N, C, respectively.

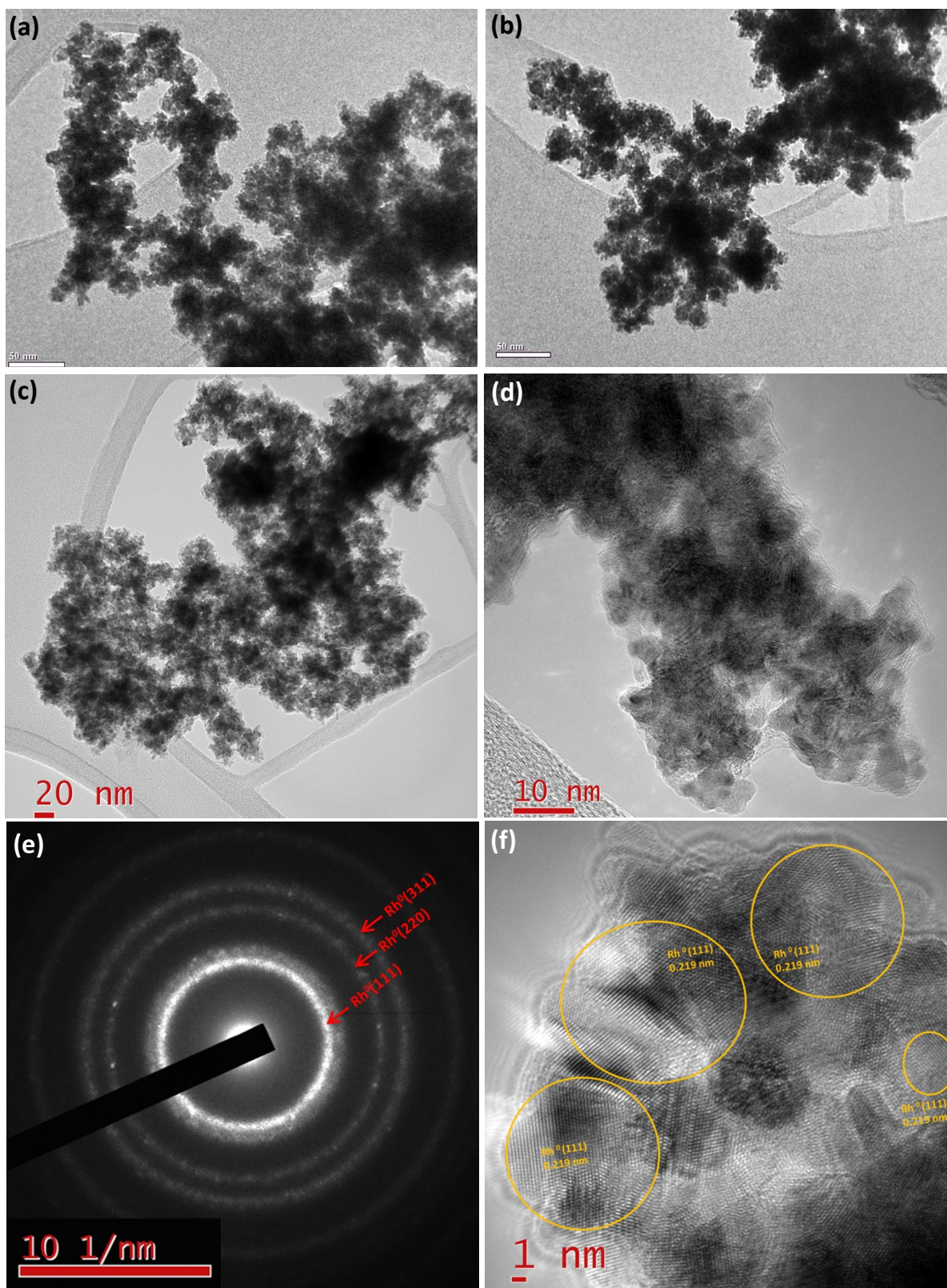


Figure S4. (a-d) TEM images of RhNPs/C sample showing the presence of ultra-small RhNPs. (e) SAED profile of RhNPs/C composite. (f) HRTEM image of RhNPs/C.

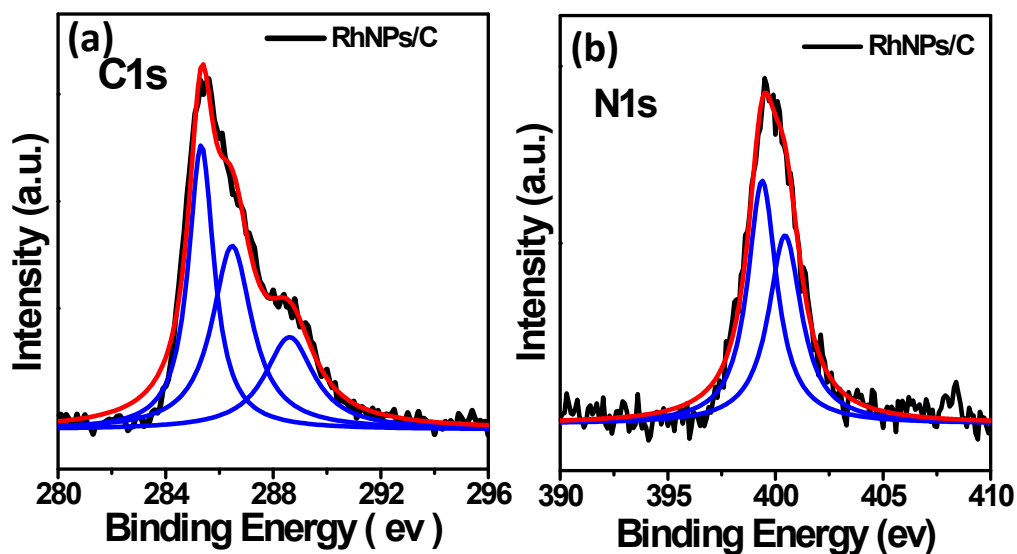


Figure S5. XPS spectra of (a) C1s spectra of RhNPs/C, (b) N1s spectra of RhNPs/C.

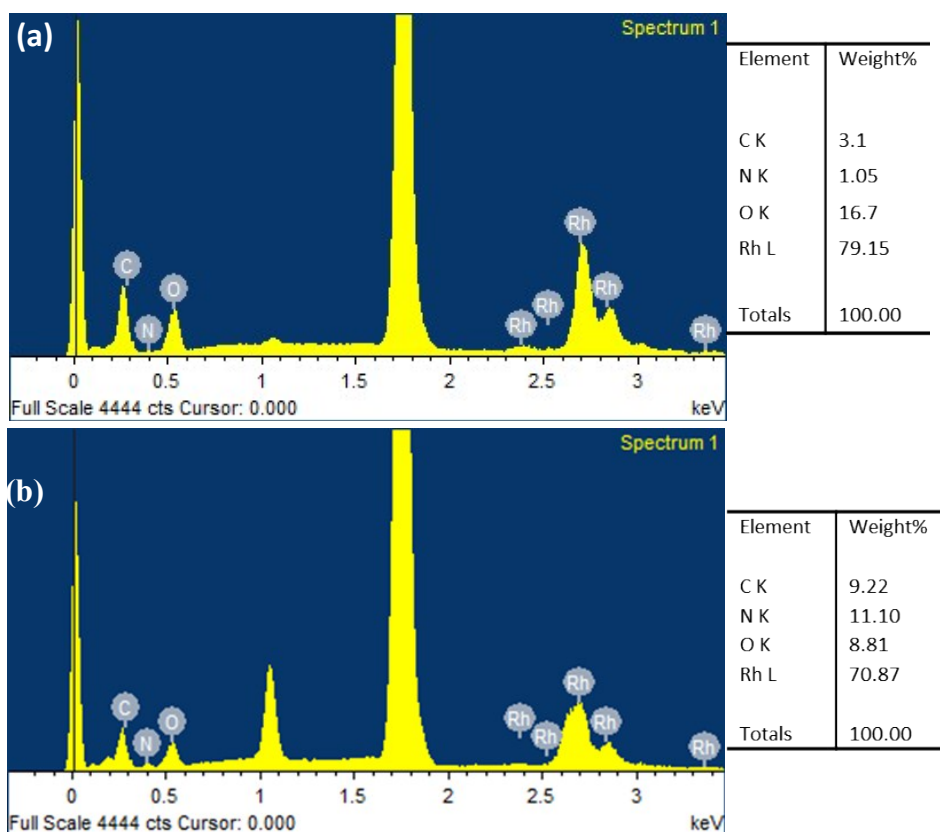


Figure S6. EDS spectrum of and corresponding weight% of Rh, C, N, O of (a) Rh-Rh₂O₃-NPs/C and (b) RhNPs/C.

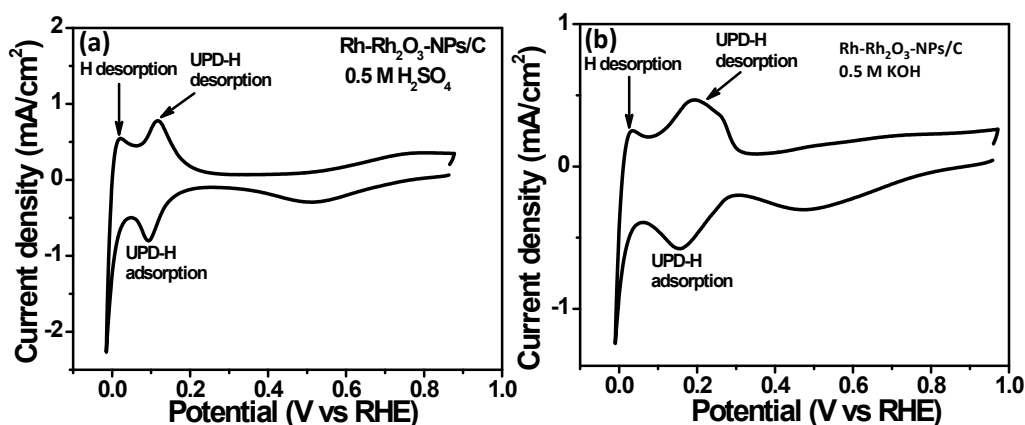


Figure S7. Cyclic voltammograms of Rh-Rh₂O₃-NPs/C showing H adsorption and desorption peaks clearly in (a) 0.5 M H₂SO₄ and (b) 0.1 M KOH. All experiments were performed at 30 mV/sec scan rate in the N₂ atmosphere.

Electrochemically active surface area (ECSA) calculation:

Electrochemically active surface area (ECSA) was calculated by following equation³:

$$ECSA = S/m \times v \times c$$

Where S is double layer corrected total area under hydrogen desorption curve or CO stripping curve, v is the scan rate (V/s), c is the required charge to oxidize a monolayer of hydrogen or CO on the rhodium surface (mCcm⁻²). The value of c is 0.21 mCcm⁻² for UPD-H and 0.42 mCcm⁻² for CO stripping, m is the Rh loading on the electrode surface (mg).

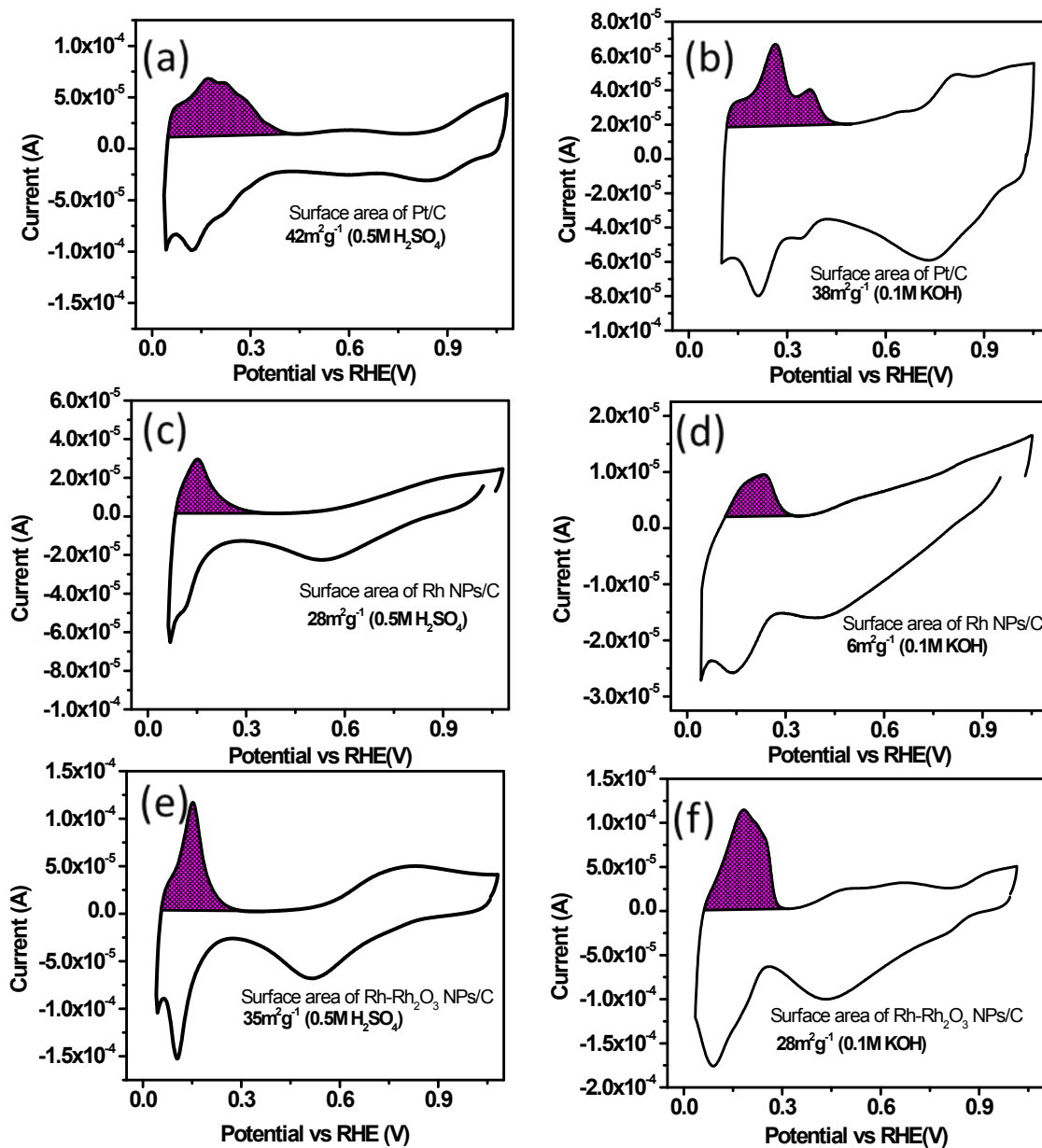


Figure S8. ECSA was calculated from UPD-H region of different catalysts in acid and base solutions. (a,b) CVs of comm. Pt/C in 0.5 M H₂SO₄, 0.1 M KOH solutions. (c,d) CVs of comm. RhNPs/C in 0.5 M H₂SO₄, 0.1 M KOH solutions. (e,f) CVs of Rh-Rh₂O₃-NPs/C in 0.5 M H₂SO₄, 0.1 M KOH solutions. The shaded area was taken for ECSA calculation.

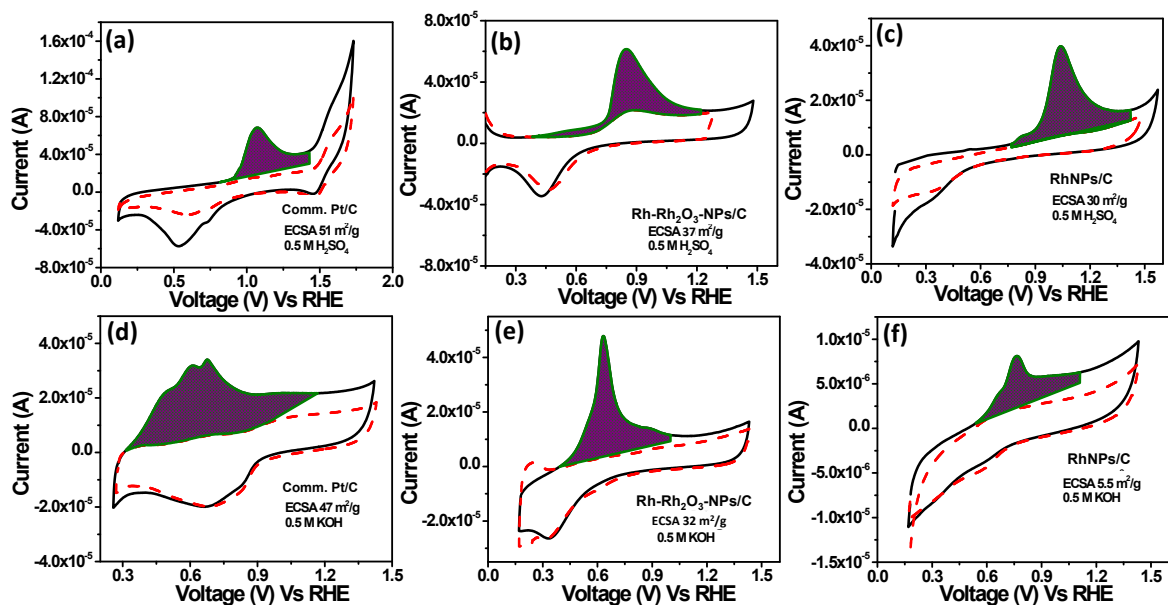


Figure S9. ECSA calculation from CO stripping: (a-c) CVs of comm. Pt/C, comm. Rh/C, Rh-Rh₂O₃-NPs/C and RhNPs/C in 0.5 M H₂SO₄. (d-f) CVs of comm. Pt/C, comm. Rh/C, Rh-Rh₂O₃-NPs/C and RhNPs/C in 0.5 M KOH. The shaded area was taken for ECSA calculation.

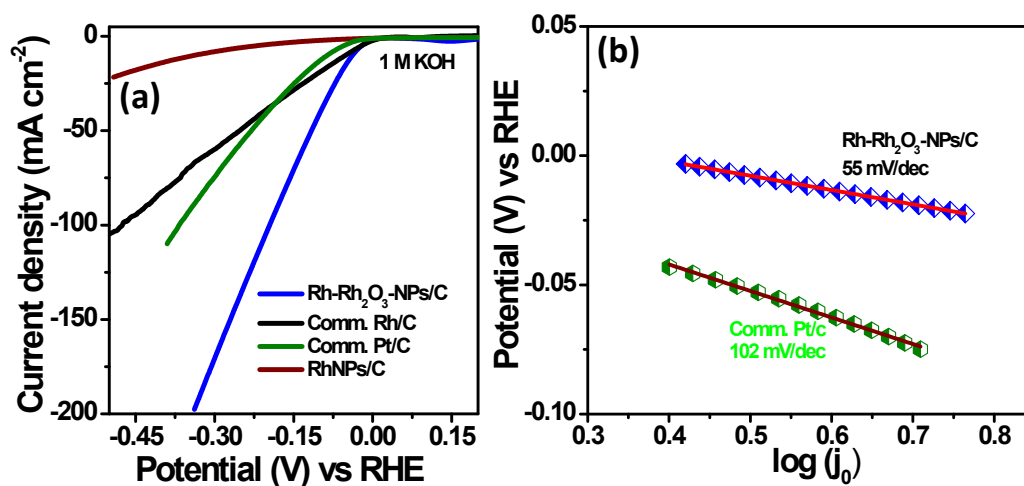


Figure S10. (a) HER activity of Rh-Rh₂O₃-NWs/C, comm. Rh/C, comm. Pt/C and RhNPs/C in 1 M KOH. (b) Tafel plot of Rh-Rh₂O₃-NPs/C and comm. Pt/C for 1 M KOH.

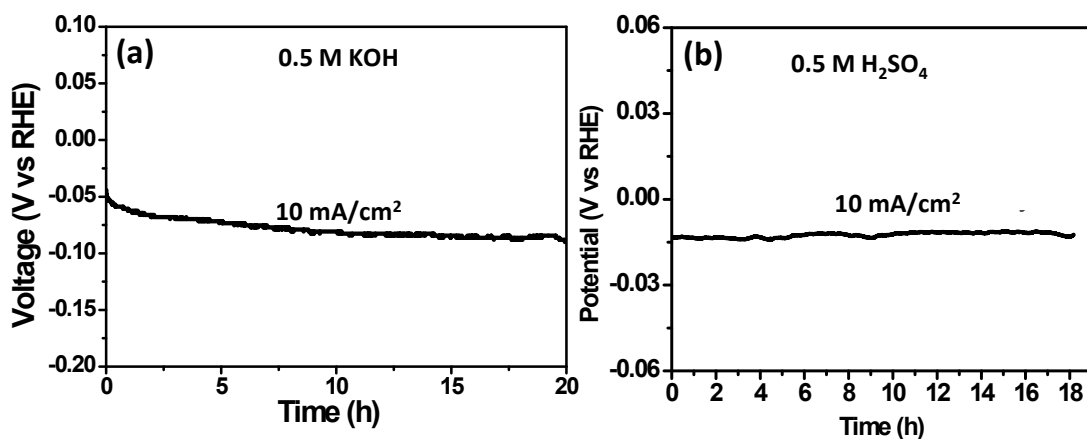


Figure S11. (a, b) Chronopotentiometric stability of Rh-Rh₂O₃-NPs/C in 0.5 M H₂SO₄ and 0.5 M KOH for 18 hours

Table S1. Different HER parameters of Rh-Rh₂O₃-NPs/C, comm. Pt/C, RhNPs/C and comm. Rh/C catalysts in 0.5 M KOH and 0.5 M H₂SO₄ solutions.

| Solution | Catalyst | Overpotential (mV) At (10 mA cm ⁻²) | Current density at -0.1 V (RHE) | SA (mAcm ⁻² _{Rh}) at -0.1 V (RHE) | MA (Ag ⁻¹) at -0.1 V (RHE) | Tafel slope (mV/dec) | Exchange current density (i ₀) (mAcm ⁻²) |
|--|---|--|---------------------------------|--|--|----------------------|--|
| 0.5 KOH | M Rh-Rh ₂ O ₃ -NPs/C | 63 | 20.5 | 2.56 | 0.72 | 113 | 1.5 |
| | comm. Pt/C | 103 | 9.5 | 0.87 | 0.33 | 70 | 1.3 |
| | RhNPs/C | 228 | 2.5 | 1.45 | 0.0875 | - | - |
| | comm. Rh/C | 150 | 5 | 1.45 | 0.17 | 116 | 0.9 |
| 0.5 H₂SO₄ | M Rh-Rh ₂ O ₃ -NPs/C | 13 | 96 | 9.6 | 3.4 | 32 | 4.2 |
| | comm. Pt/C | 24 | 67 | 5.58 | 2.35 | 34 | 2.28 |
| | RhNPs/C | 18 | 71 | 8.87 | 2.485 | 39 | 2.8 |
| | comm. Rh/C | 55 | 29 | 6.76 | 1.015 | 50 | 0.96 |

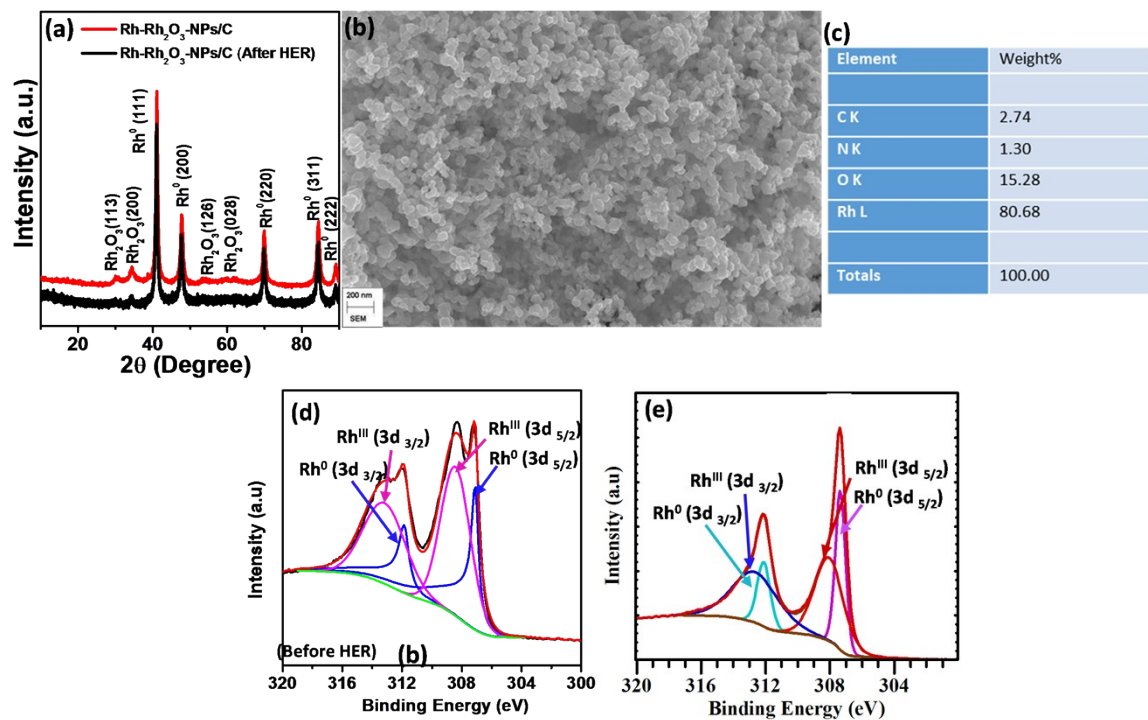


Figure S12. (a) p-XRD pattern of Rh-Rh₂O₃-NPs/C before and after HER stability in 0.5 M H₂SO₄ medium. (b, c) FESEM image and EDS measurement after HER stability. (d,e) XPS survey scan of Rh3d, O1s after chronopotentiometric stability test for 12 h.

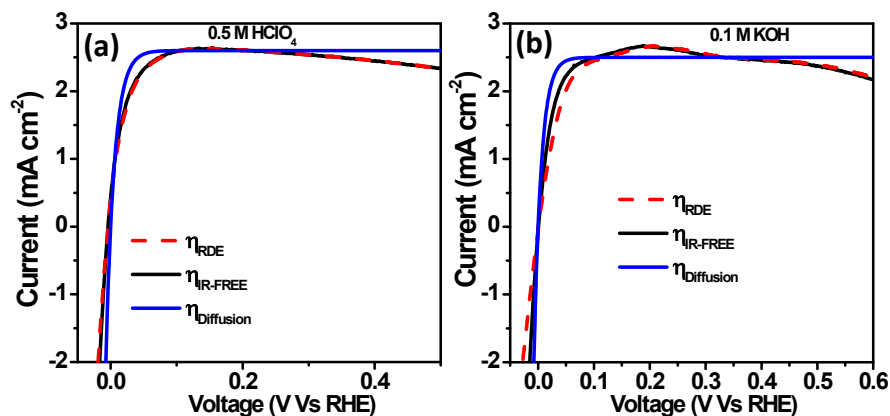


Figure S13. (a, b) iR corrected and diffusion current corrected polarization curve in 0.5 M HClO₄ and 0.1 M KOH.

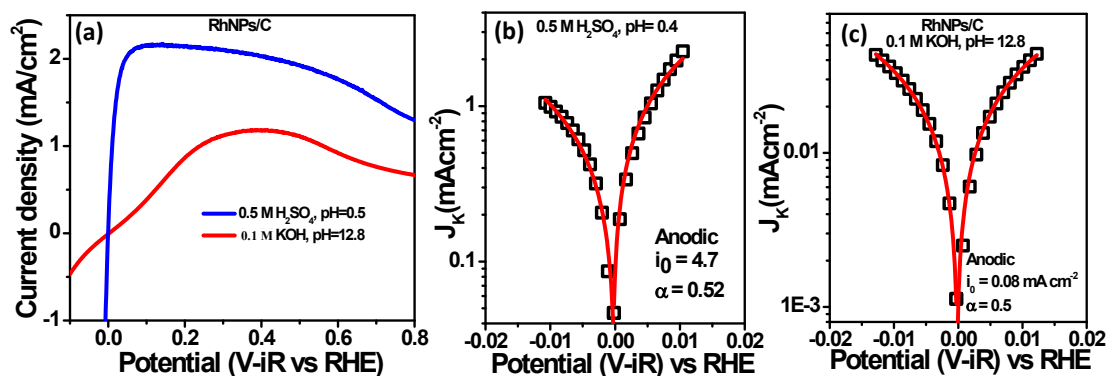


Figure S14. (a) HER/HOR polarization curves (positive going direction) on RhNPs/C catalyst in 0.5 M H₂SO₄ and 0.1 M KOH solution saturated with H₂ (~1 atm). (a, b) Kinetic current vs iR-corrected potential plot (Butler-Volmer plot) of RhNPs/C catalyst at 0.5 M H₂SO₄ and 0.1 M KOH was shown.

Table S2. Kinetic parameters of Rh-Rh₂O₃-NPs/C and RhNPs/C catalyst extracted from the Butler-Volmer fitting for acid and base solutions.

| | Solution | Exchange Current density (i_0) (mAcm ⁻²) | Specific Exchange Current density (i_0) (mAcm ⁻² _{metal}) | Specific exchange current (A mg ⁻¹) | Anodic transfer coefficient (α_a) | Cathodic transfer coefficient (α_c) |
|---|--------------------------------------|--|--|---|--|--|
| Rh-Rh₂O₃-NPs/C | 0.5 M HClO ₄ | 4.3±0.2 | 0.43 | 150±28 | 0.55 | 0.45 |
| | 0.1 M KOH | 3.4±0.2 | 0.425 | 119±28 | 0.52 | 0.48 |
| RhNPs/C | 0.5 M H ₂ SO ₄ | 4.7±0.2 | 0.58 | 164±35 | 0.52 | 0.48 |
| | 0.1 M KOH | 0.08±0.01 | 0.04 | 2.8±0.14 | 0.5 | 0.5 |

Table S3. Different HOR parameters of Rh-Rh₂O₃-NPs/C, RhNPs/C catalyst for acid and alkaline media.

| Catalyst | Solution | Exchange current density (i_0) (mAcm ⁻²) | Specific exchange Current (A mg ⁻¹) | Anodic transfer coefficient (α) | Cathodic transfer coefficient (α) |
|--|--------------------------------------|--|---|--|--|
| Rh-Rh ₂ O ₃ -NPs/C | 0.5 M HClO ₄ | 4.3±0.2 | 150±28 | 0.55 | 0.45 |
| | 0.1 M HClO ₄ | 4.8±0.2 | 168±30 | 0.55 | 0.45 |
| | 0.1 M H ₂ SO ₄ | 4.8±0.2 | 163±29 | 0.5 | 0.5 |
| | 0.5 M KOH | 3.5±0.2 | 118±25 | 0.55 | 0.45 |
| | 0.1 M KOH | 3.4±0.2 | 119±28 | 0.52 | 0.48 |
| RhNPs/C | 0.5 M H ₂ SO ₄ | 4.7±0.2 | 164±35 | 0.52 | 0.48 |
| | 0.1 M H ₂ SO ₄ | 4.9±0.2 | 171±36 | 0.55 | 0.45 |
| | 0.1 M HClO ₄ | 4.0±0.2 | 141±33 | 0.55 | 0.45 |
| | 0.1 M KOH | 0.08±0.01 | 2.8±0.14 | 0.5 | 0.5 |

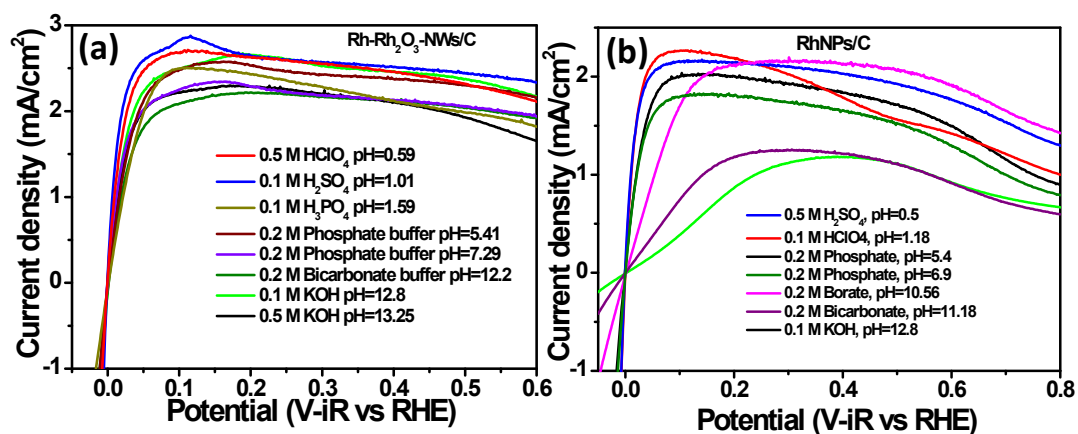


Figure S15. Positive going HOR polarization curves at 10 mV/sec scan rate with 1600 rpm rotation of (a) Rh-Rh₂O₃-NPs/C and (b) RhNPs/C in H₂ saturated different buffer solutions. All polarization curves are iR corrected accordingly.

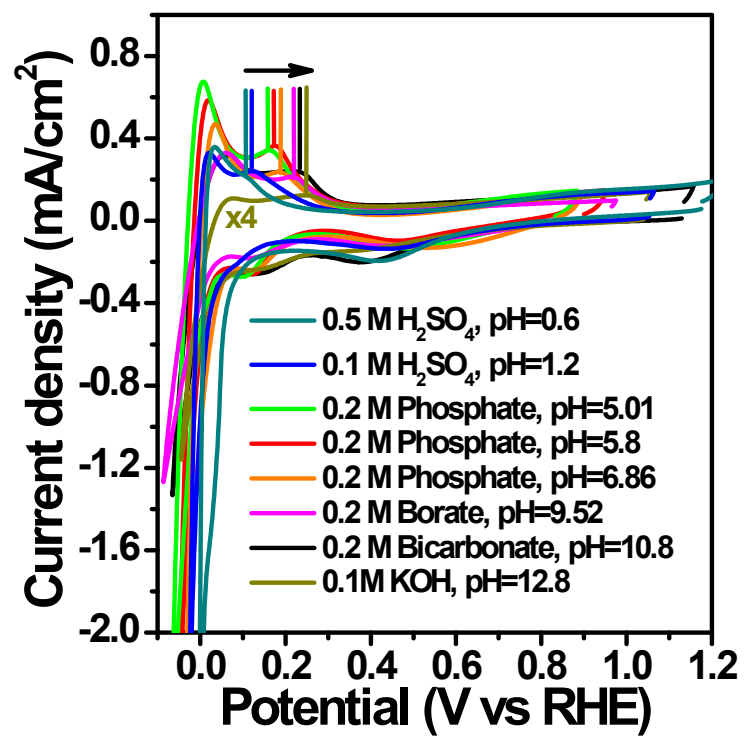


Figure S16. CVs of RhNPs/C catalyst at different buffer solutions at 30 mV/sec scan rate in N₂ saturated electrolyte.

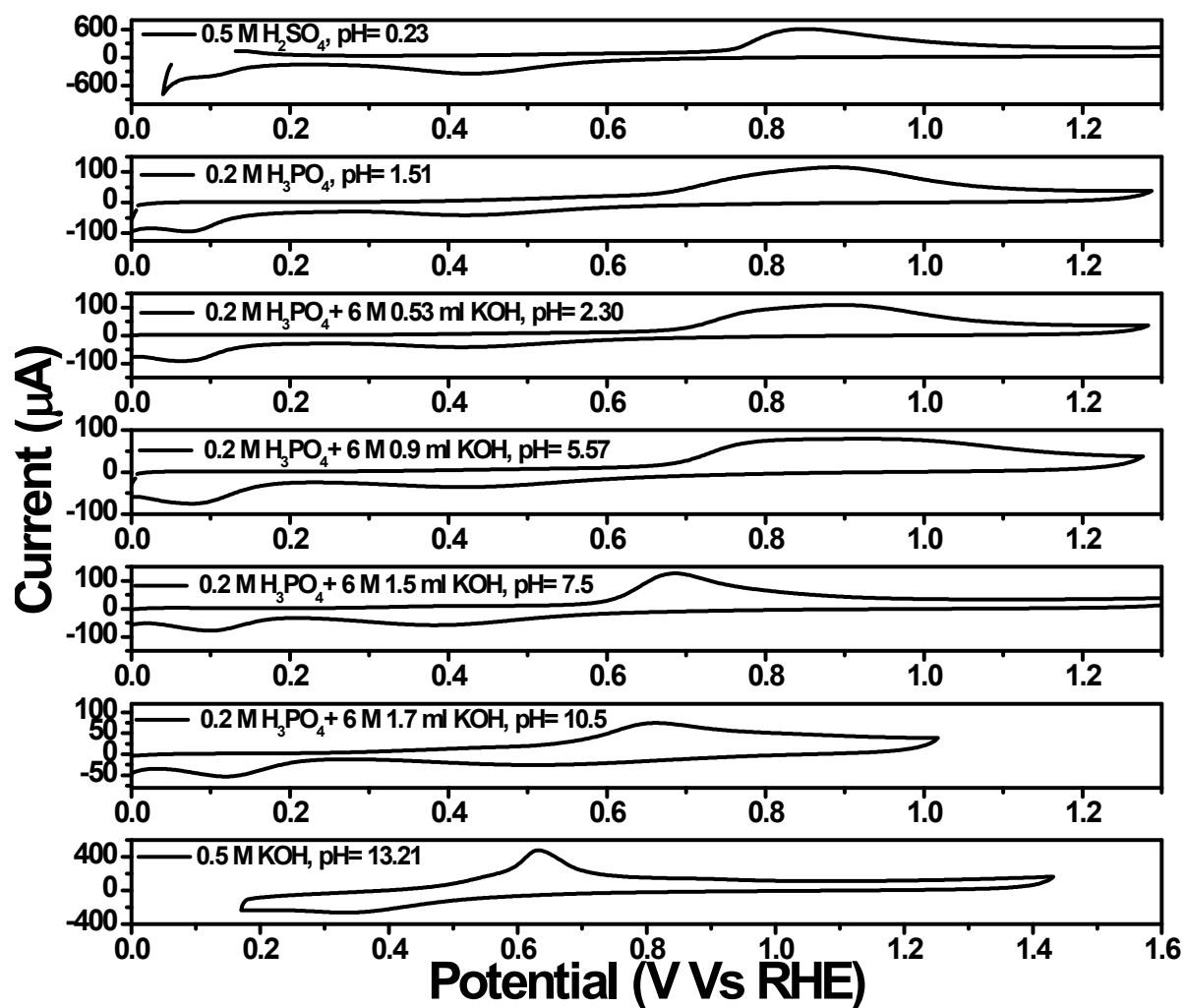


Figure S17. CO stripping voltammograms of Rh-Rh₂O₃-NPs/C catalyst in different pH solutions.

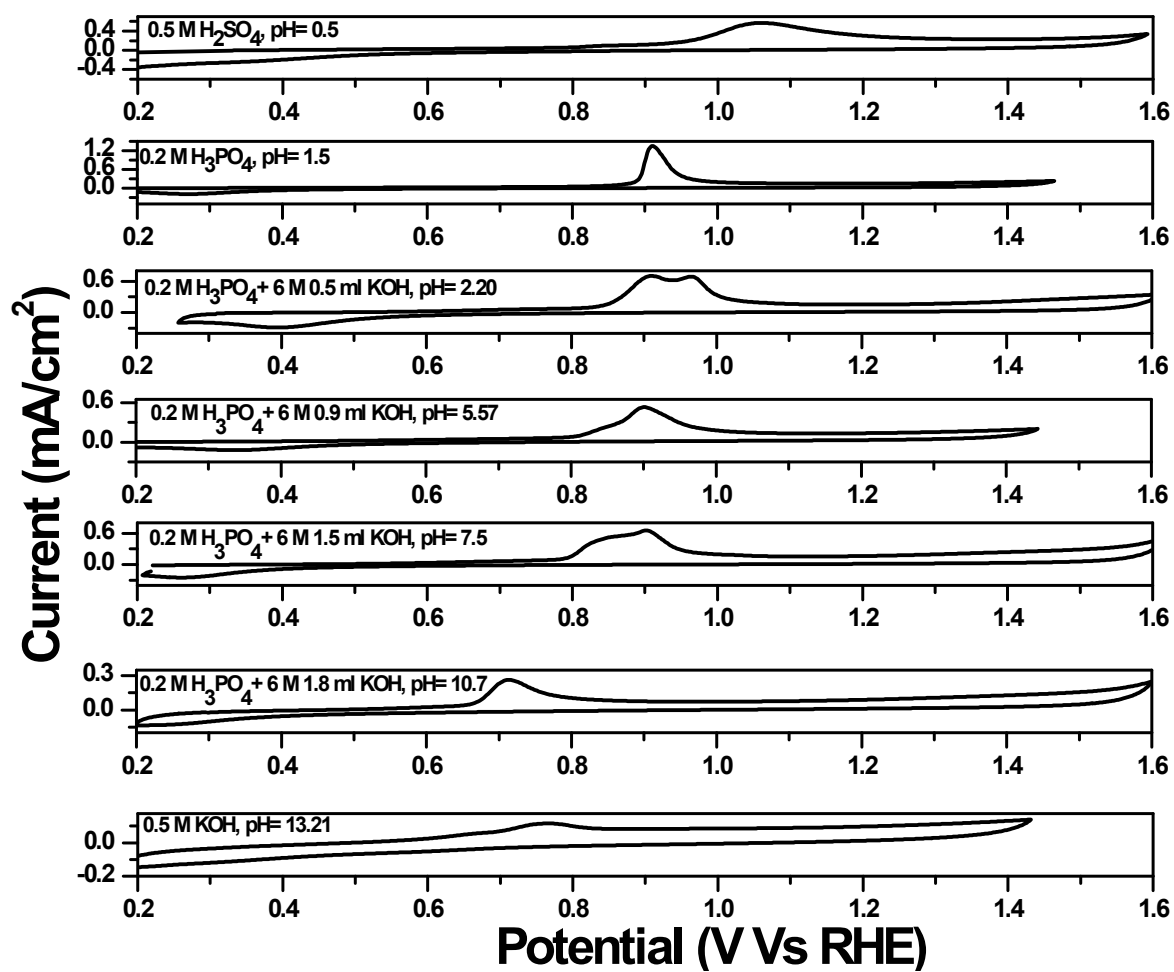


Figure S18. CO stripping voltammograms of RhNPs/C in different pH solutions.

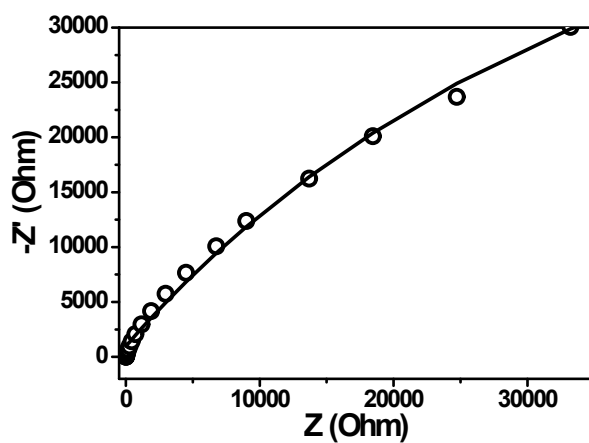


Figure S19. Nyquist plot for CN_x in 0.5 M KOH at -20 mV (RHE).

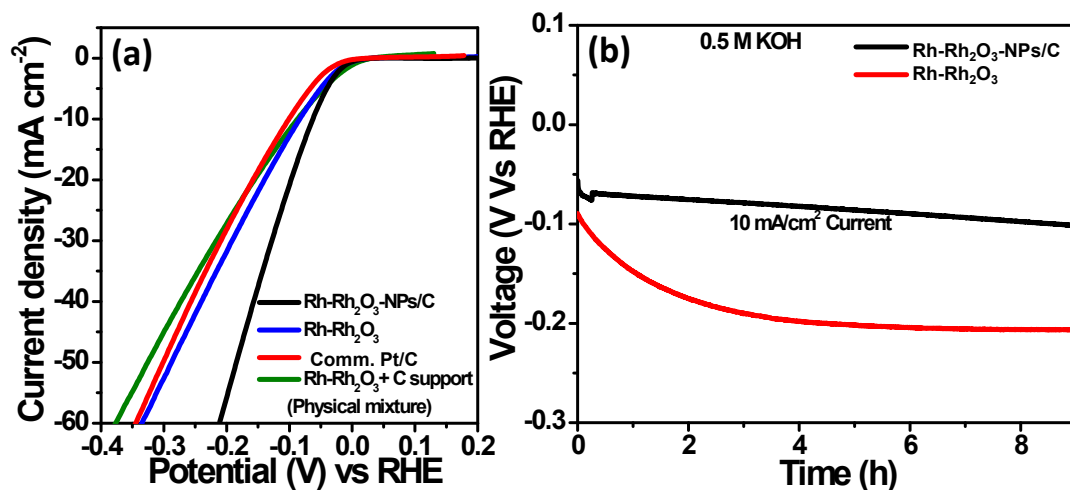


Figure S20. (a) HER activity of Rh-Rh₂O₃-NPs/C, Rh-Rh₂O₃ (without Carbon support) and comm. Pt/C in 0.5 M KOH. Rh-Rh₂O₃ was prepared by following the same synthesis procedure but no nitrogen-doped carbon was added. (b) Chronopotentiometric response at 10 mAcm⁻² current of Rh-Rh₂O₃-NPs/C and Rh-Rh₂O₃ in 0.5 M KOH showing very poor stability of Rh-Rh₂O₃.

Table S4. Comparison of HER activity of Rh-Rh₂O₃-NPs/C catalyst in alkaline medium with other reported catalysts.

| Catalyst | Catalyst loading (mg cm ⁻²) | Onset potential (mV Vs RHE) | Over potential (mV Vs RHE) vs current density (mA cm ⁻²) | Tafel slope (mV/dec) | Exchange current (mAcm ⁻²) | References |
|--|---|-----------------------------|--|----------------------|--|--|
| CoP/CC | | | 209 (10 mA cm ⁻²) | 129 | | J. Am. Chem. Soc. 2014 , 136, 7587. |
| CoN _x /C | 2.0 | -30 | 170 (10 mA cm ⁻²) | 75 | - | Nat. Commun. 2015 , 6, 7992. |
| NiP ₂ NS/CC | | -74 | 102 (10 mA cm ⁻²) | 64 | | Nanoscale 2014 , 6, 13440. |
| Co _{0.59} Fe _{0.62} P | 0.35 | -39 | 92 (10 mA cm ⁻²) | 72 | 0.568 | Nanoscale 2015 , 7, 11055. |
| Pt NWs/SLNi(OH) ₂ | 0.016 | -0 | 65 (10 mA cm ⁻²) | | | Nat. Commun. 2015 , 6, 6430. |
| Pt ₃ Ni ₂ NWs-S/C | 0.0153 | - | 50 (10 mA cm ⁻²) | - | - | Nat. Commun. 2017 , 8, 14580. |
| NiO/Ni-CNT | 0.28 | - | 80 (10 mA cm ⁻²) | 82 | - | Nat. Commun. 2014 , 5, 4695. |
| CoO _x @CN | | | 232 (10 mA cm ⁻²) | | | J. Am. Chem. Soc. 2015 , 137, 2688. |
| Porous Pd-CN _x | 0.043 | -75 | 180 (5 mA cm ⁻²) | 150 | 0.037 | ACS Catal. 2016 , 6, 1929. |
| Ni/MWCNT | - | - | 220 (20 mA cm ⁻²) | 102 | 0.011 | J. Power Sources 2014 , 266, 365. |
| Co-NRCNTs | | -(50-100) | 370 (10 mA cm ⁻²) | | | Angew. Chem. Int. Ed. 2014 , 126, 4461. |
| Mo ₂ C | 0.8 | -110 | 190 (10 mA cm ⁻²) | 54 | 0.0038 | Angew. Chem. Int. Ed. 2012 , 51, 12703. |
| 1D-RuO ₂ -CN _x | 0.012 | -16 | 95 (10 mA cm ⁻²) | 70 | 0.28 | ACS Appl. Mater. Interfaces 2016 , 8 (42), 28678. |
| Ni-Mo nanopowders | 1 | 0 | 80 (10 mA cm ⁻²) | | | ACS Catal. 2013 , 3 (2), 166. |
| Rh nanosheets RhNSs | 0.015 | 0 | 37 (10 mA cm ⁻²) (iR corrected) | 74.7 | | Chem. Mater. 2017 , 29, 5009. |
| Rh concave tetrahedra (Rh CTs) | 0.015 | 0 | 66 (10 mA cm ⁻²) (iR corrected) | 117.7 | | Chem. Mater. 2017 , 29, 5009. |
| Rh tetrahedra (Rh THs) | 0.015 | 0 | 64 (10 mA cm ⁻²) (iR corrected) | 79.5 | | Chem. Mater. 2017 , 29, 5009. |
| Rh-Rh ₂ O ₃ -NPs/C | 0.028 | 0 | 63 (10 mA cm ⁻²) 81 (20 mA cm ⁻²) | 70 | 1.5 | This work |

Table S5. Comparison of HER activity of Rh-Rh₂O₃-NPs/C catalyst in acidic medium with other reported catalysts.

| Catalyst | Catalyst loading (mg cm ⁻²) | Onset potential (mV Vs RHE) | Over potential (mV Vs RHE) vs current density (mA cm ⁻²) | Tafel slope (mV/de c) | Exchange current (mAcm ⁻²) | References |
|--|---|-----------------------------|--|-----------------------|--|---|
| NiAu/Au | - | -7 | - | 36 | - | J. Am. Chem. Soc. 2015 , <i>137</i> , 5859. |
| Au-aerogel-CN _x | 0.127 | -30 | -225 (20 mA cm ⁻²) | 53 | 0.03 | J. Mater. Chem. A 2015 , <i>3</i> , 23120. |
| A-Ni-C | | - | -34 (10 mA cm ⁻²) | 41 | 1.2 | Nat. Commun. 2016 , <i>7</i> , 10667. |
| 1D-RuO ₂ -CN _x | 93 | -14 | -93 (10 mA cm ⁻²) | 40 | 0.22 | ACS Appl. Mater. Interfaces 2016 , <i>8</i> , 28678. |
| Pd-CN _x | 0.043 | -12 | 55 | 35 | 0.40 | ACS Catal. 2016 , <i>6</i> , 1929. |
| Pt ₁₃ Cu ₇₃ Ni ₁₄ /CN F @CF | | 5 | 70 | 38 | | ACS Appl. Mater. Interfaces 2016 , <i>8</i> , 3464 |
| Pt _{tripods} @PAA | 81 | +19.6 | -25(90 mA cm ⁻²) | - | - | ACS Catal. 2017 , <i>7</i> , 452. |
| NiMoN _x /C | 0.25 | -78 | - | 35.9 | 0.24 | Angew. Chem. Int. Ed. 2012 , <i>51</i> , 6131. |
| MoS ₂ /CoSe ₂ | 0.28 | -11 | -68 (10 mA cm ⁻²) | 36 | 0.073 | Nat. Commun. 2015 , <i>6</i> , 5982. |
| WPNA/CC | 2 | -50 | -130 (10 mA cm ⁻²) | 69 | 0.29 | ACS Appl. Mater. Interfaces 2014 , <i>6</i> , 21874. |
| MoP-CA2 | 0.36 | -40 (IR free) | -125 (10 mA/cm ²) | 54 | 0.086 | Adv. Mater. 2014 , <i>26</i> , 5702. |
| Nano MoP | 1 | - | -110 (10 mA cm ⁻²) | 45 | 0.12 | Chem. Mater. 2014 , <i>26</i> , 4826. |
| (GO 8 wt%) Cu-MOF | 0.226 | -87 | -400 (122.48 mA cm ⁻²) | 84 | - | Adv. Funct. Mater. 2013 , <i>23</i> , 5363. |
| NiP ₂ NS/CC | 4.3 | -50 | -75 (10 mA cm ⁻²) | 51 | 0.26 | Nanoscale 2014 , <i>6</i> , 13440. |
| Co-NRCNT | 0.28 | -50 | -260 (10 mA cm ⁻²) | 69 | 0.01 | Angew. Chem. Int. Ed. 2014 , <i>126</i> , 4461. |
| CoSe ₂ | 0.37 | -30 | -90 (4 mA cm ⁻²) | 40 | 0.037 | Energy Environ. Sci. 2013 , <i>6</i> , 3553. |
| CoP/CC | 0.92 | -38 | 67 (10 mA cm ⁻²) | 51 | 0.288 | J. Am. Chem. Soc. 2014 , <i>136</i> , 7587 |
| CoN _x /C | 2 | -20 | 133 | 57 | 0.07 | Nat. Commun. 2015 , <i>6</i> , 7992. |
| Co _{0.6} Mo _{1.4} N ₂ | 0.24 | | -200 (10 mA cm ⁻²) | | 0.23 | J. Am. Chem. Soc. 2013 , <i>135</i> , 19186. |
| MoS ₂ /RGO | 0.28 | -100 | - | -41 | | J. Am. Chem. Soc. 2011 , <i>133</i> , 7296. |
| Ni ₂ P | | -25 | -130 (20 mA cm ⁻²) | -46 | 0.033 | J. Am. Chem. Soc. 2013 , <i>135</i> , 9267. |
| Ni-Mo-N nanosheets | 0.25 | -78 | ~ -200 mV (3.5 mA cm ⁻²) | 35.9 | 0.24 | Angew. Chem. Int. Ed. 2012 , <i>51</i> , 6131. |
| Rh/SiNWs | 0.056 | - | -44(0.1 mA cm ⁻²) | 24 | 0.008 | Nat. Commun. 2016 , <i>7</i> , 12272. |
| Rh-Ag-SiNW-2 | 0.140 | - | 120 (10 mA cm ⁻²) | 51 | 0.087 | J. Mater. Chem. A 2017 , <i>5</i> , 1623. |
| Rh-MoS ₂ | 0.309 | - | 47 (10 mA cm ⁻²) | 24 | 0.1142 | Adv Funct. Mater. 2017 , <i>27</i> , 1700359. |
| Rh-Rh ₂ O ₃ -NPs/C | 0.028 | 0 | -14 (10 mA cm ⁻²) | 32 | 4.2 | This Work. |

References:

1. Barman, S.; Sadhukhan, M. *J. Mater. Chem.* **2012**, *22*, 21832-21837.
2. Kundu, M. K.; Bhowmik, T.; Barman, S. *J. Mater. Chem. A* **2015**, *3*, 23120-23135
3. Sadhukhan, M.; Kundu, M. K.; Bhowmik, T.; Barman, S. *Int. J. Hydrogen Energy* **2017**, *42*, 9371-9383.